

Supporting Material

Effect of MgAl-Layered Double Hydroxide Exchanged with Linear Alkyl Carboxylates on Fire retardancy of PMMA and PS

Calistor Nyambo¹, Ponusa Songtipya^{2,3}, E.Manias², Maria M. Jimenez-Gasco,³Charles A. Wilkie^{1*}

¹ Department of Chemistry, Marquette University, Milwaukee, WI 53201-1881, USA

² Department of Materials Science and Engineering, ³ Plant Pathology Department, Penn State University, University Park, PA, USA.

The d-spacing increases monotonously with the chain length of the surfactant, as is shown in **Figure S1**.

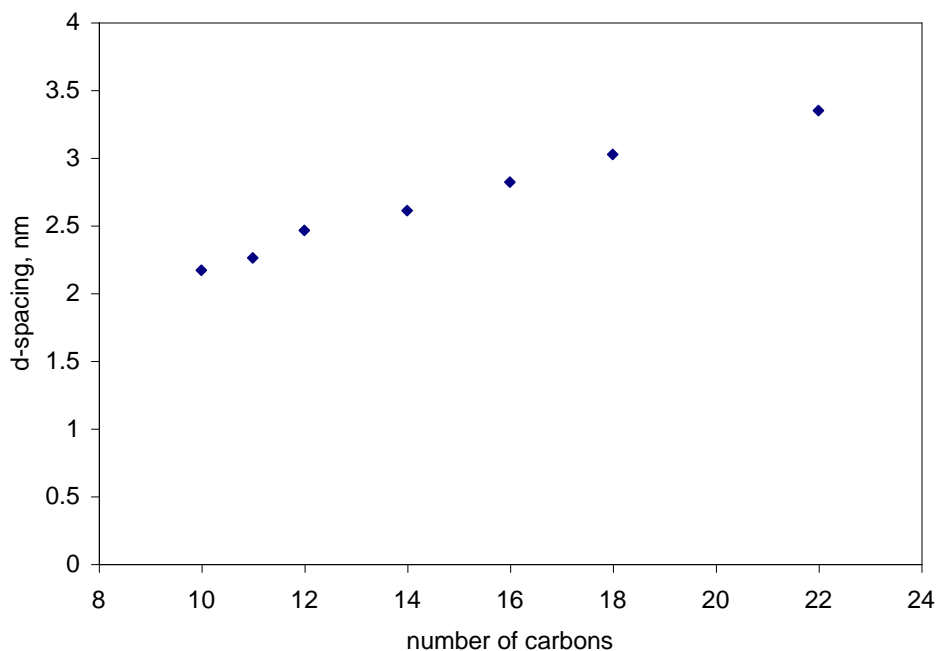


Figure S1 Plot of d-spacing vs. number of carbons for the MgAl –LDHs exchanged from MgAl-NO₃⁻ LDH

Here are shown all of the XRD traces. In the case of the C10 surfactant, no peak is seen, indicative of some disorder, and in the other cases, a peak is seen at lower values

of 2θ, likely indicating that some amount of intercalation occurs. The XRD data for the PMMA – LDH systems is collected in Table S1.

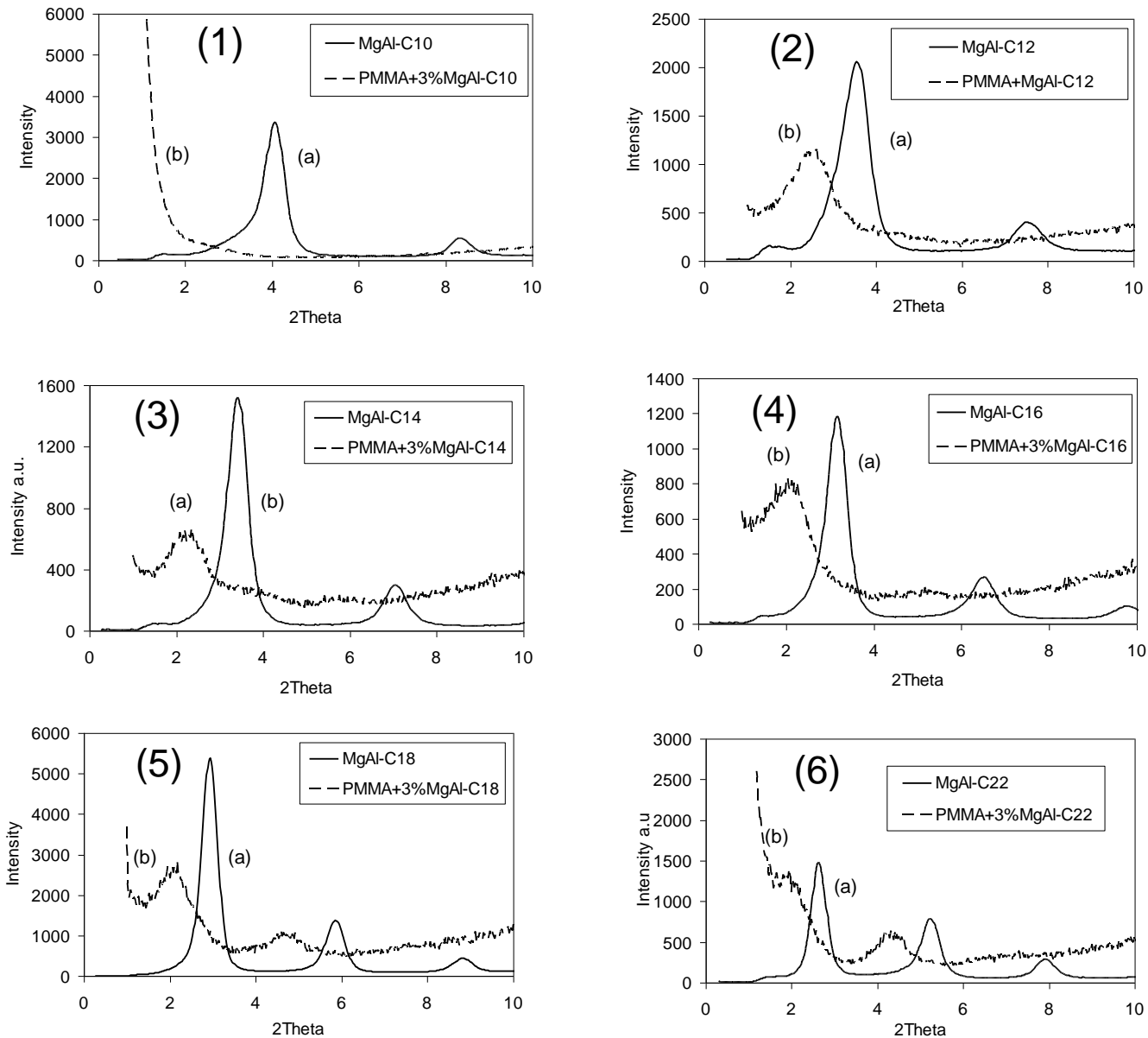
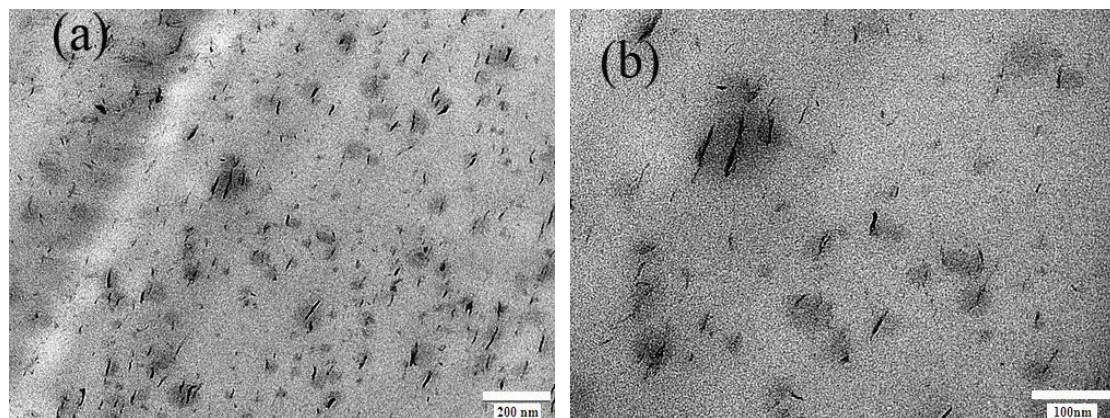


Figure S2 XRD traces for (1) (a) MgAl-C10 LDH and (b) PMMA+MgAl-10 LDH, (2) (a) MgAl-12 LDH and (b) PMMA+MgAl-C12 LDH, (3) (a)MgAl-C14 LDH, (b) PMMA+MgAl-C14, (4) (a)MgAl-C16 LDH, (b) PMMA+MgAl-C16, (5) (a) MgAl-C18 LDH (b) PMMA+MgAl-C18 LDH, and (6) (a)MgAl-C22, (b)PMMA+MgAl-C22 LDH.

Table S1 XRD data for PMMA + MgAl-LDHs composites. 2θ is the angle of the d_{003} diffraction peak, d the corresponding basal spacing, and Δd the change in basal spacing for the composite compared to the respective organo-LDH (positive Δd denotes expansion/intercalation) .

Formulation	2θ	d – spacing (\AA)	Δd - spacing (\AA)
PMMA+3%MgAl-C10	–	–	–
PMMA+3%MgAl-C12	2.62	33.7	+9.1
PMMA+3%MgAl-C14	2.38	37.1	+11.0
PMMA+3%MgAl-C16	2.18	40.5	+12.3
PMMA+3%MgAl-C18	2.12	41.6	+11.5
PMMA+3%MgAl-C22	1.96	45.0	+11.5

Representative TEM images of some of the PMMA-LDH nanocomposites are shown in the paper. Here we provide the remaining TEM images in Figure S3. These clearly show good nanodispersion and the presence of either individual clay platelets or, at worst, a small number of platelets together. These PMMA-LDH systems are all true nanocomposites and should probably be described as mixed intercalated – exfoliated systems.



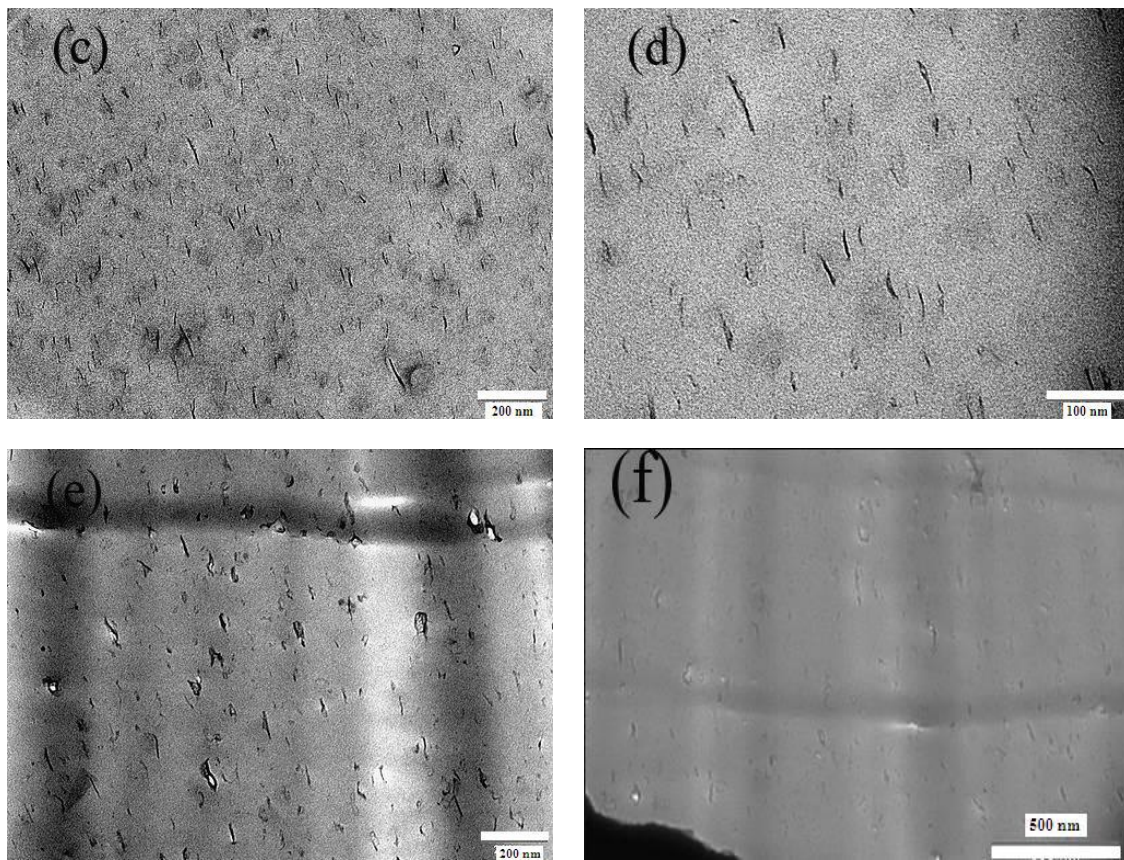


Figure S3 TEM images at (a) low and (b) high magnification for PMMA+3%MgAl-C12, (c) low and (d) high magnification for PMMA+3%MgAl-C14 , and (e) low and (f) high magnification for PMMA+3%MgAl-C22 . The scale bars for low and high magnification are indicated on the images.

The XRD traces for the PS-LDH system are shown in **Figure S4**. Only with the C10 surfactant is a peak seen at lower values of 2θ and this is weaker and broader than that of the clay alone. In all other cases, either a weak and broad peak is seen at about the same value of 2θ or else no peak is seen. The observation of a weaker and broader peak or no peak is an indication of disorder, which could be either disorder leading to exfoliation or microcomposite-type disorder and the latter is expected in this system.

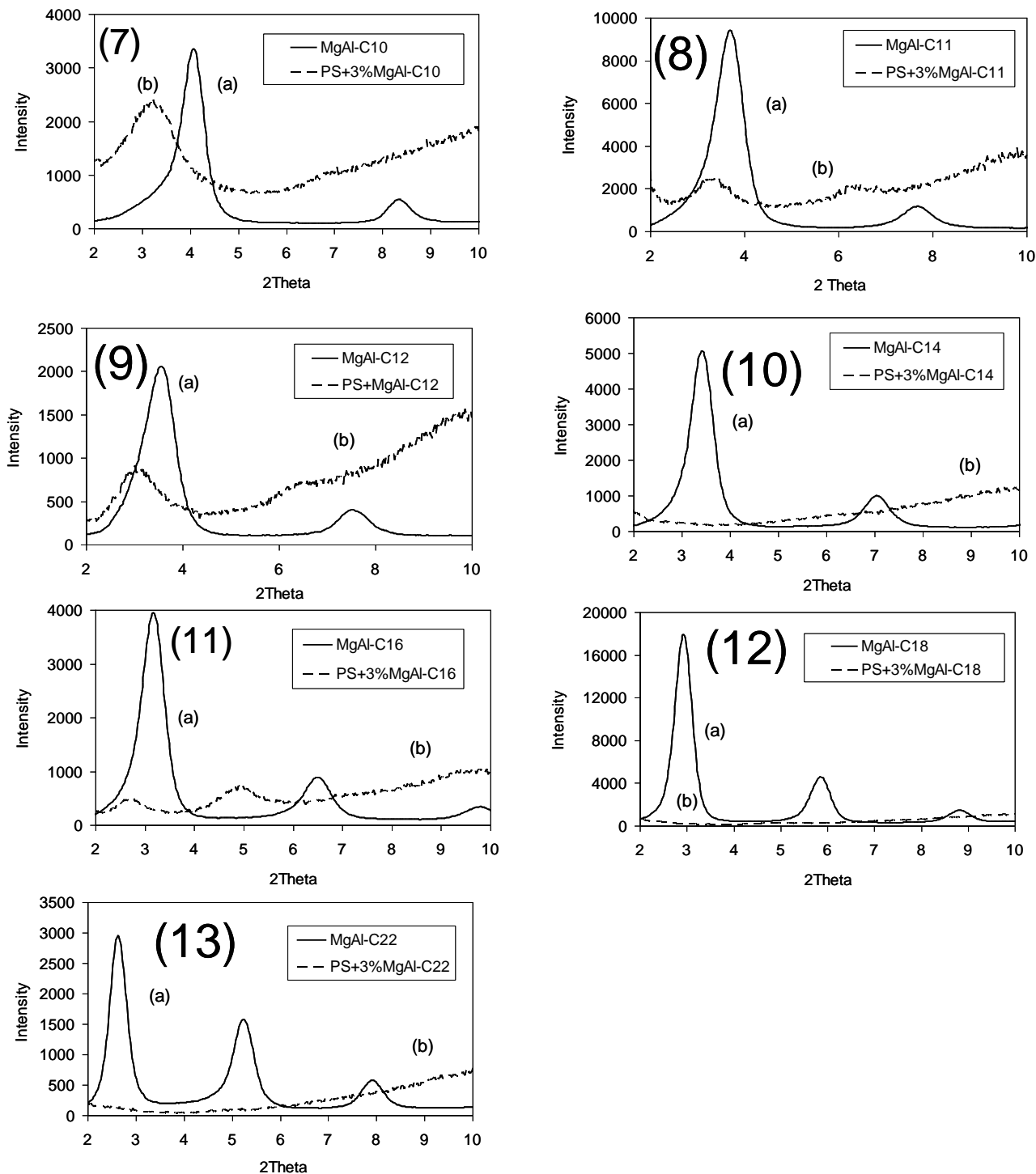
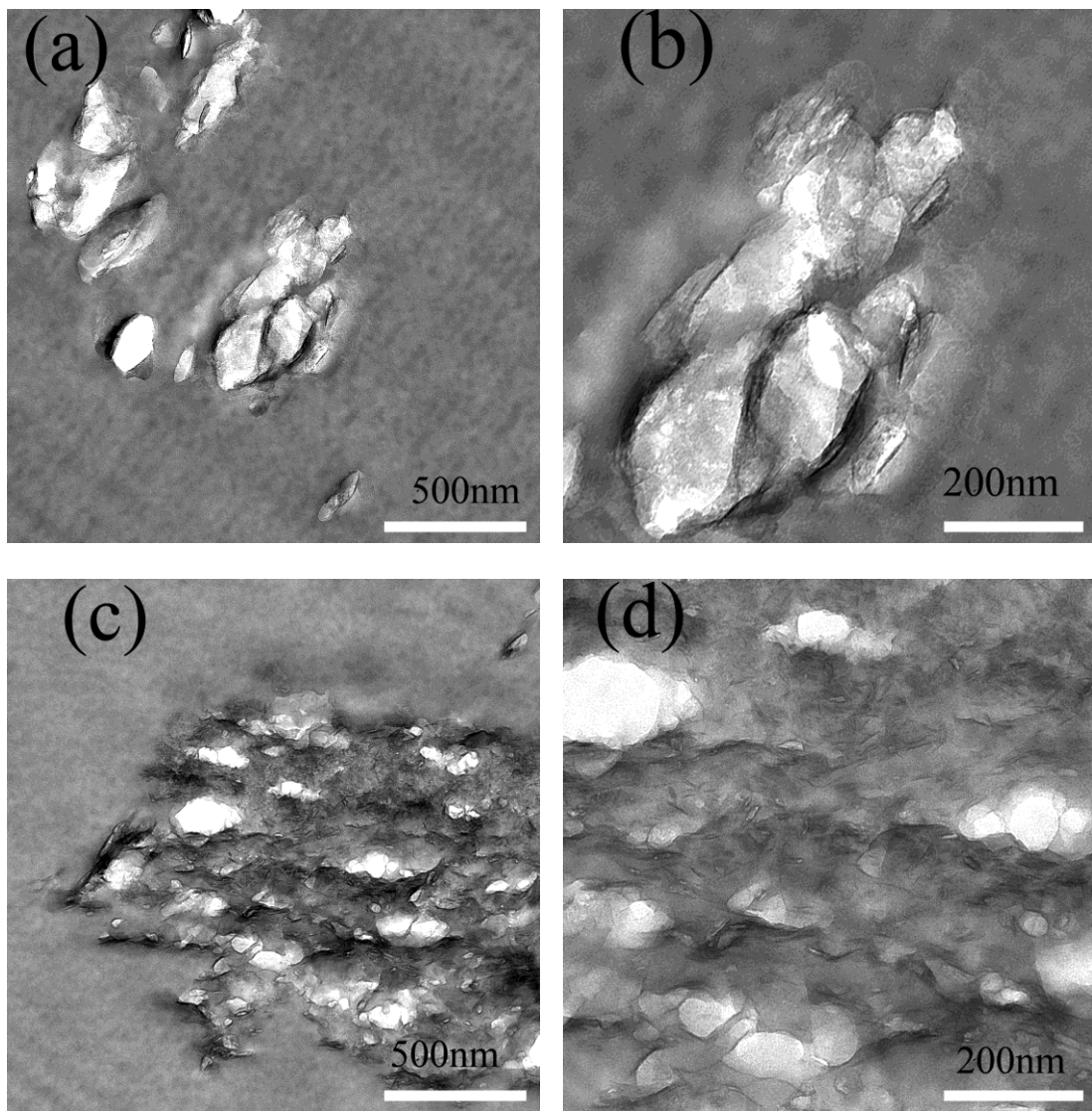


Figure S4 XRD traces for (7) (a) MgAl-C10 LDH and (b) PS+MgAl-10 LDH, (8) (a) PS+MgAl-11 LDH and (b) PS+MgAl-C11 LDH, (9) (a) PS+MgAl-12 LDH and (b) PS+MgAl-C12 LDH, (10) (a) MgAl-C14 LDH, (b) PS+MgAl-C14, (11) (a) MgAl-C16 LDH, (b) PS+MgAl-C16, (12) (a) MgAl-C18 LDH (b) PS+MgAl-C18 LDH, and (13) (a) MgAl-C22, (b) PS+MgAl-C22 LDH.

The TEM images of two of the PS-LDH systems were shown in the paper and the remaining images are given here as **Figure S5**. The presence of very large tactoids is obvious in these figures and these must be described as microcomposites. The dispersion is clearly poor on the nanometer level and one can even question if it is good micrometer dispersion.



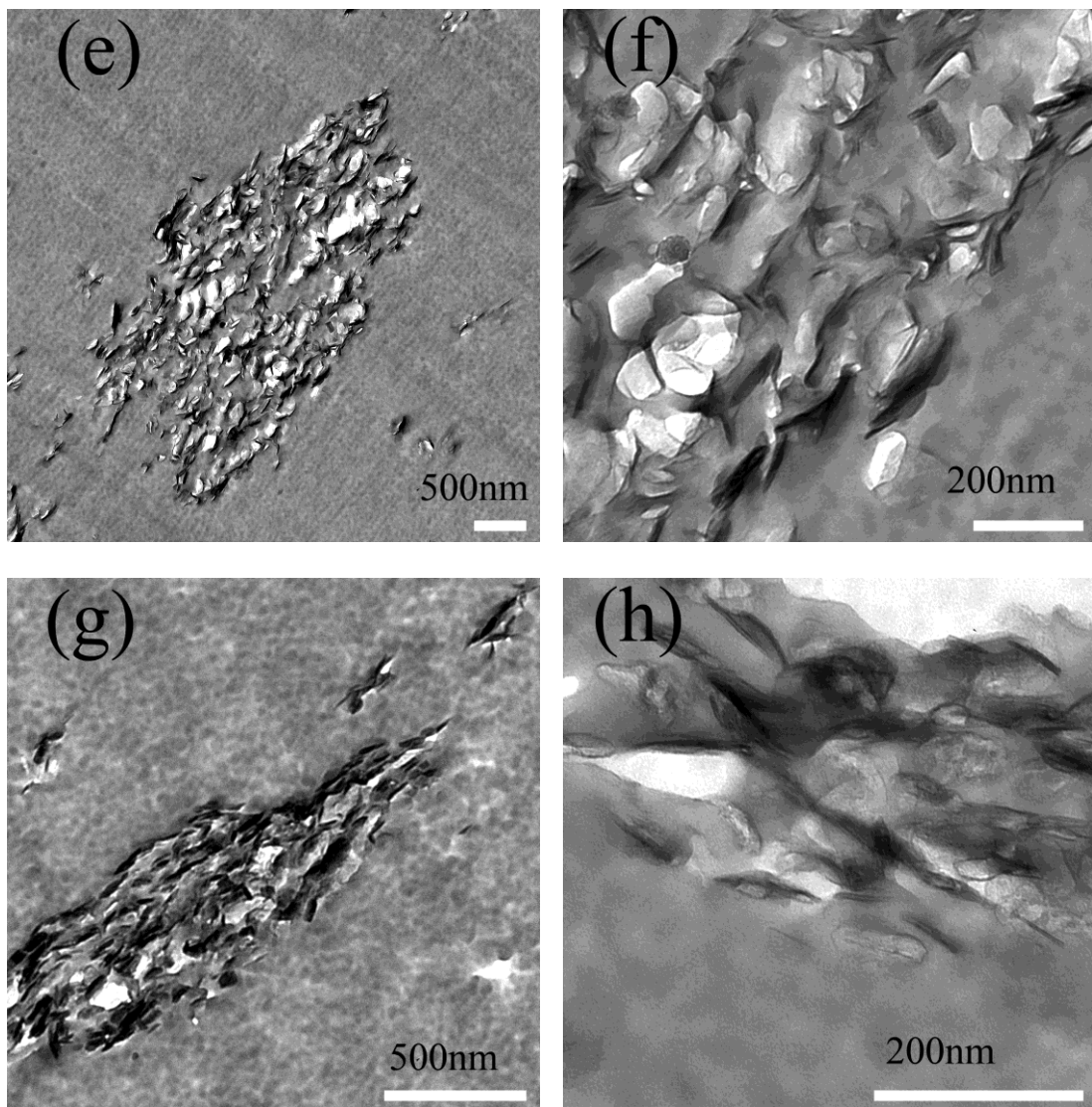


Figure S5 TEM images at (a) low and (b) high magnification for PS+3%MgAl-C10, (c) low and (d) high magnification for PS+3%MgAl-C12 , (e) low and (f) high magnification for PS+3%MgAl-14, and (g) low and (h) high magnification for PS+3%MgAl-16 . The scale bars for low and high magnification are indicated on the images.

The TGA data is presented in tabular form in the paper, here, **Figure S6**, are shown the TGA curves themselves. It is very obvious that all of the nanocomposites are more thermally stable than is virgin PMMA. In order to address the question of the importance of LDH formation versus simply the presence of aluminum and magnesium hydroxides, mixtures of PMMA with these materials have been prepared and the TGA curves are shown in **Figure S7**. The addition of the minerals does give enhanced thermal

stability to PMMA and it appears to be comparable to the enhancement seen with the LDHs.

Likewise with PS, there is enhanced thermal stability for the PS-LDH systems relative to virgin PS, as seen in **Figure S8**. Also like PMMA, the addition of ATH and/or MDH to PS also gives enhanced thermal stability, **Figure S9**.

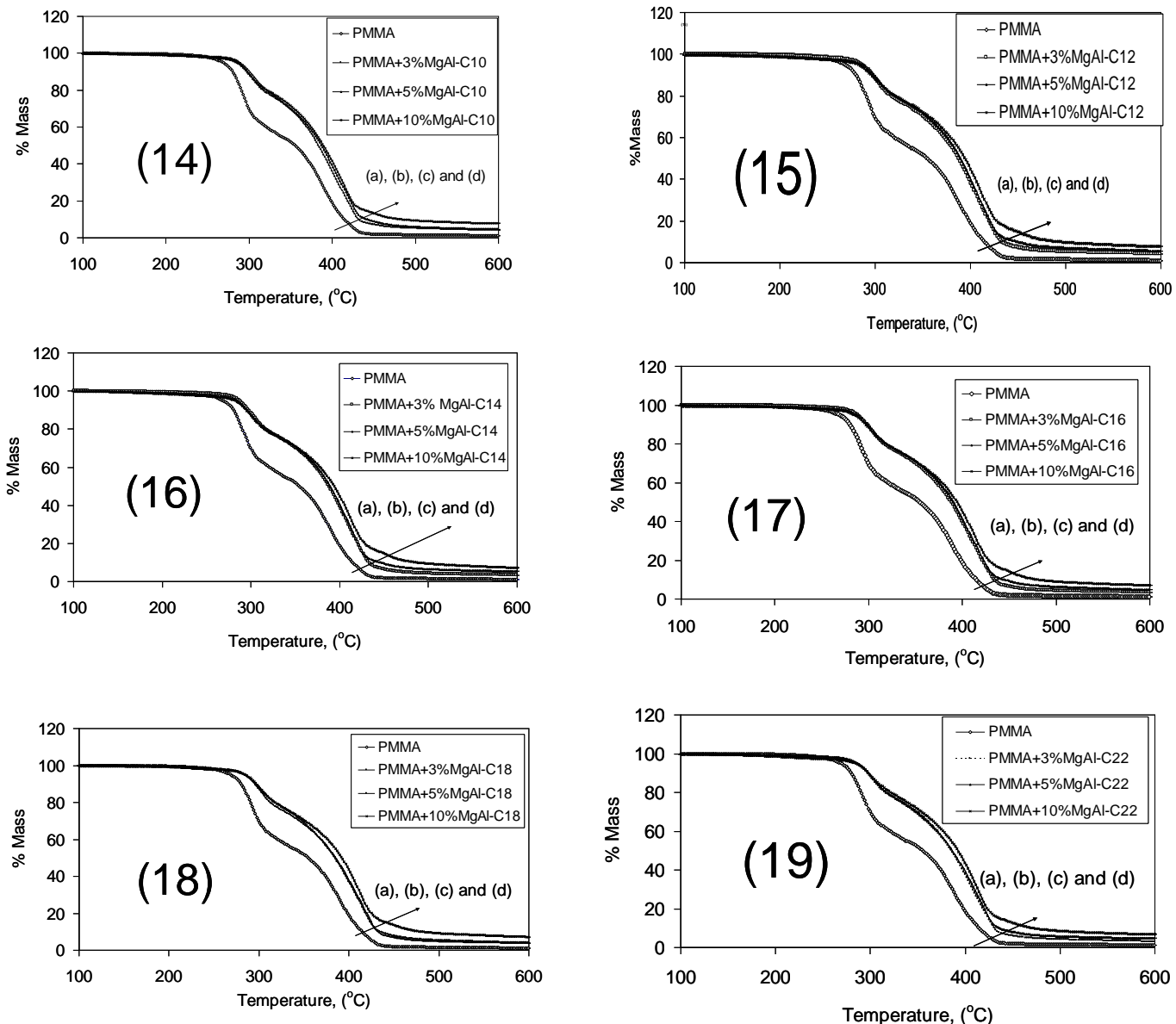


Figure S6 TGA results for PMMA with (14) MgAl-C10 LDH, (15) MgAl-C12 LDH, (16) MgAl-C14 LDH, (17) MgAl-C16, (18) MgAl-C18 LDH (19) MgAl-C22 LDH.

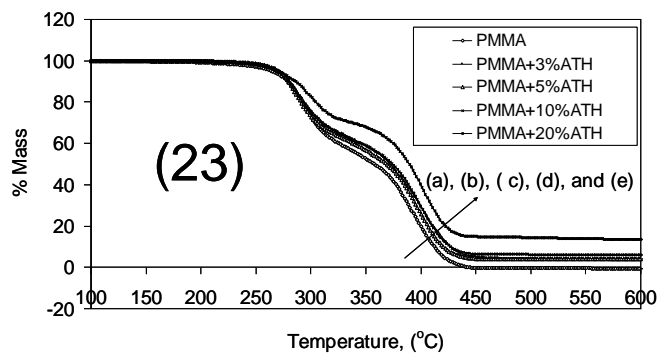
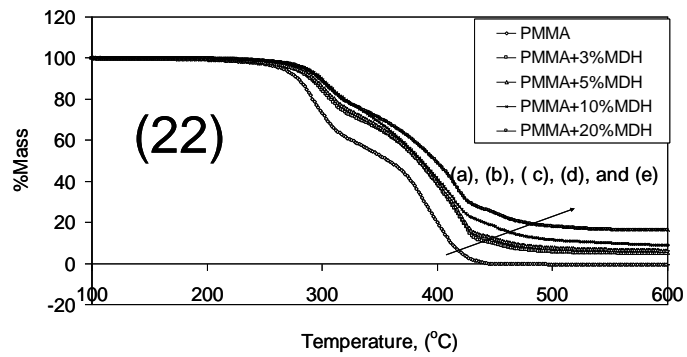
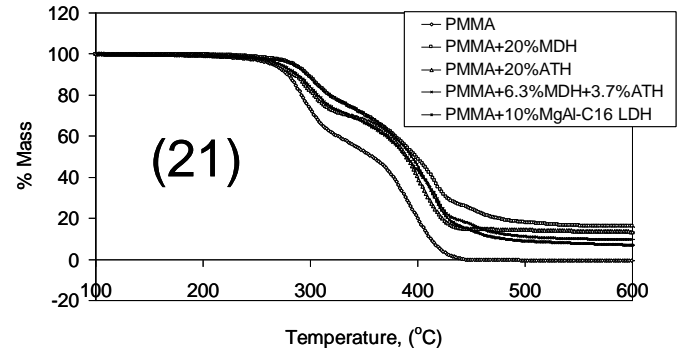
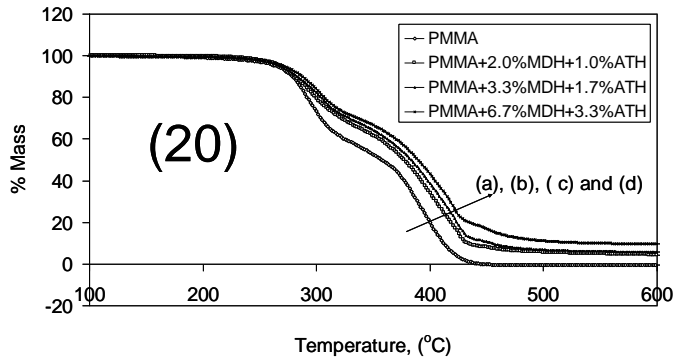


Figure S7 TGA curves for:

(20) (a)PMMA(b)PMMA+2.0%MDH+1.0%ATH(c)PMMA+3.3%MDH+1.7%ATHand(d)PMMA+6.7%MDH+3.3%ATH,

(21)TGA curves for PMMA, PMMA+10%MgAl-C16 LDH, PMMA+6.3%MDH+3.7%ATH, PMMA+20%ATH and PMMA+20%MDH

(22)TGA curves for (a) PMMA (b) PMMA+ 3%MDH, (c) PMMA+5%MDH, (d)PMMA+ 10% MDH and (e) PMMA+20% of MDH.

(23)TGA curves for (a) PMMA (b) PMMA+ 3%ATH, (c) PMMA+5%ATH, (d) PMMA+ 10% ATH and (e) PMMA+20% of ATH

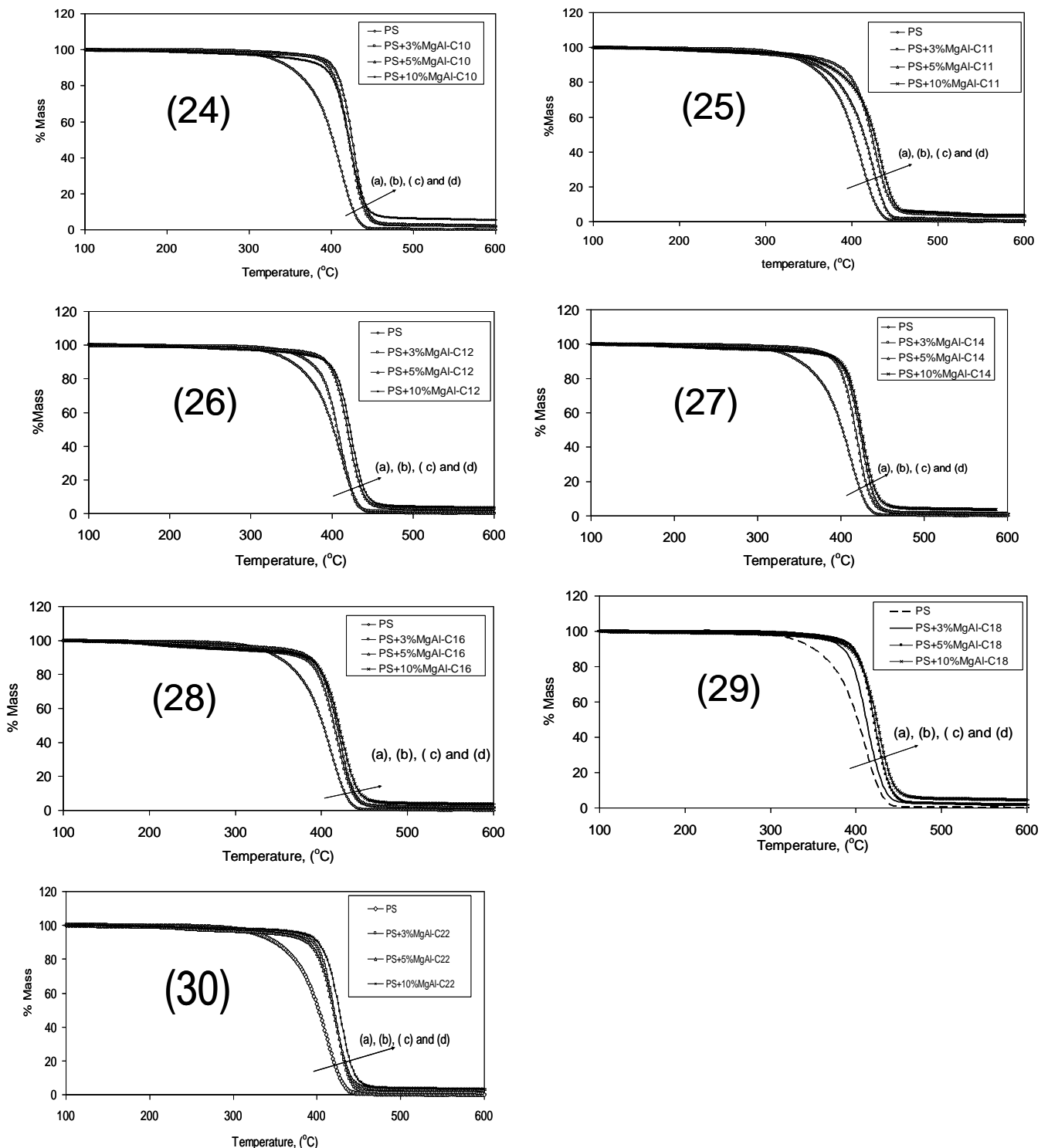


Figure S8 TGA results for PS with (24) MgAl-C10 LDH, (25)MgAl-11 LDH, (26)MgAl-C12 LDH, (27) MgAl-C14 LDH, (28) MgAl-C16 LDH, (29) MgAl-C18 and (30) MgAl-C22 LDH

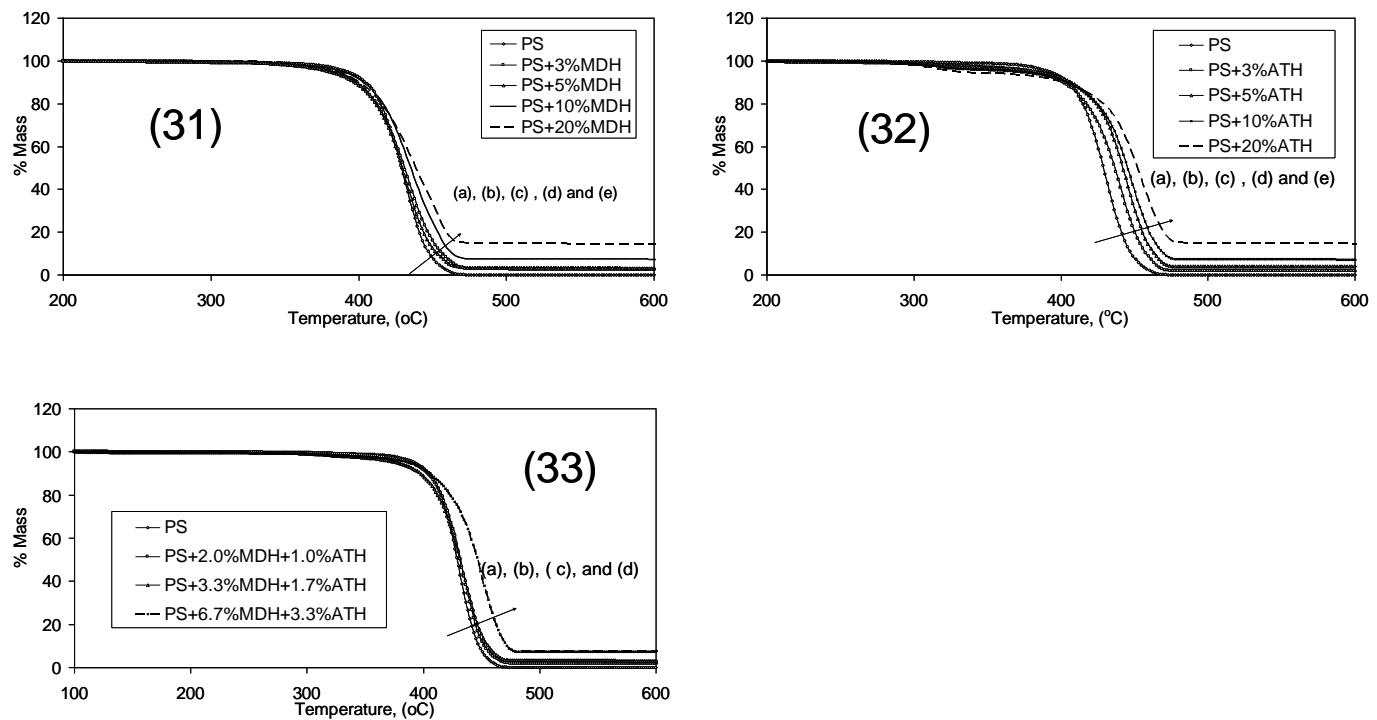


Figure S9 TGA curves for:
(31) (a) PS (b) PS+3%MDH(c) PS+5%MDH (d) PS+10%MDH (e) PS+20%MDH,
(32) (a) PS (b) PS+2%ATHH(c) PS+5%ATH (d) PS+10%ATH (e) PS+20%ATH, and
(33)(a) PS (b) PS+2.0%MDH+1.0%ATH (c) PS+3.3%MDH+1.7%ATH and
(d) PS+6.7%MDH+3.3%ATH.

All of the cone calorimetric data is presented in the paper, here we show the heat release rate curves for the various systems; PMMA-LDH systems are given in **Figure S10** while that for PS-LDH is in **Figure S11**. Here one can graphically see the complete curve rather than simply the peak value as given in the paper.

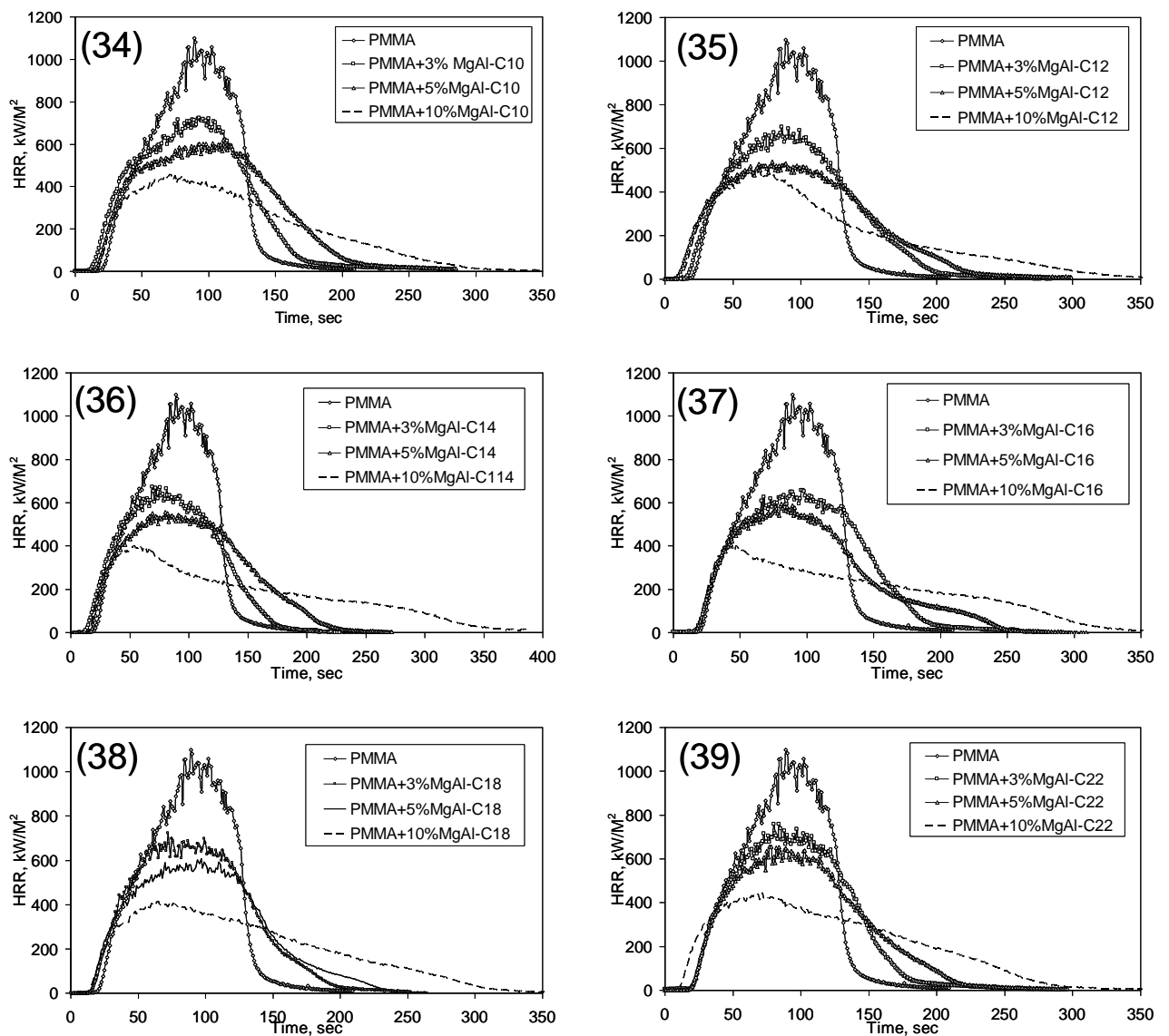


Figure S10 HRR curves for PMMA with (34)MgAl-C10 LDH, (35) MgAl-11 LDH, (36)MgAl-C12 LDH, (37) MgAl-C14 LDH, (38)MgAl-C16 LDH and (39)MgAl-C22 LDH at 3, 5 and 10% loadings obtained at $50\text{ kW}/\text{m}^2$

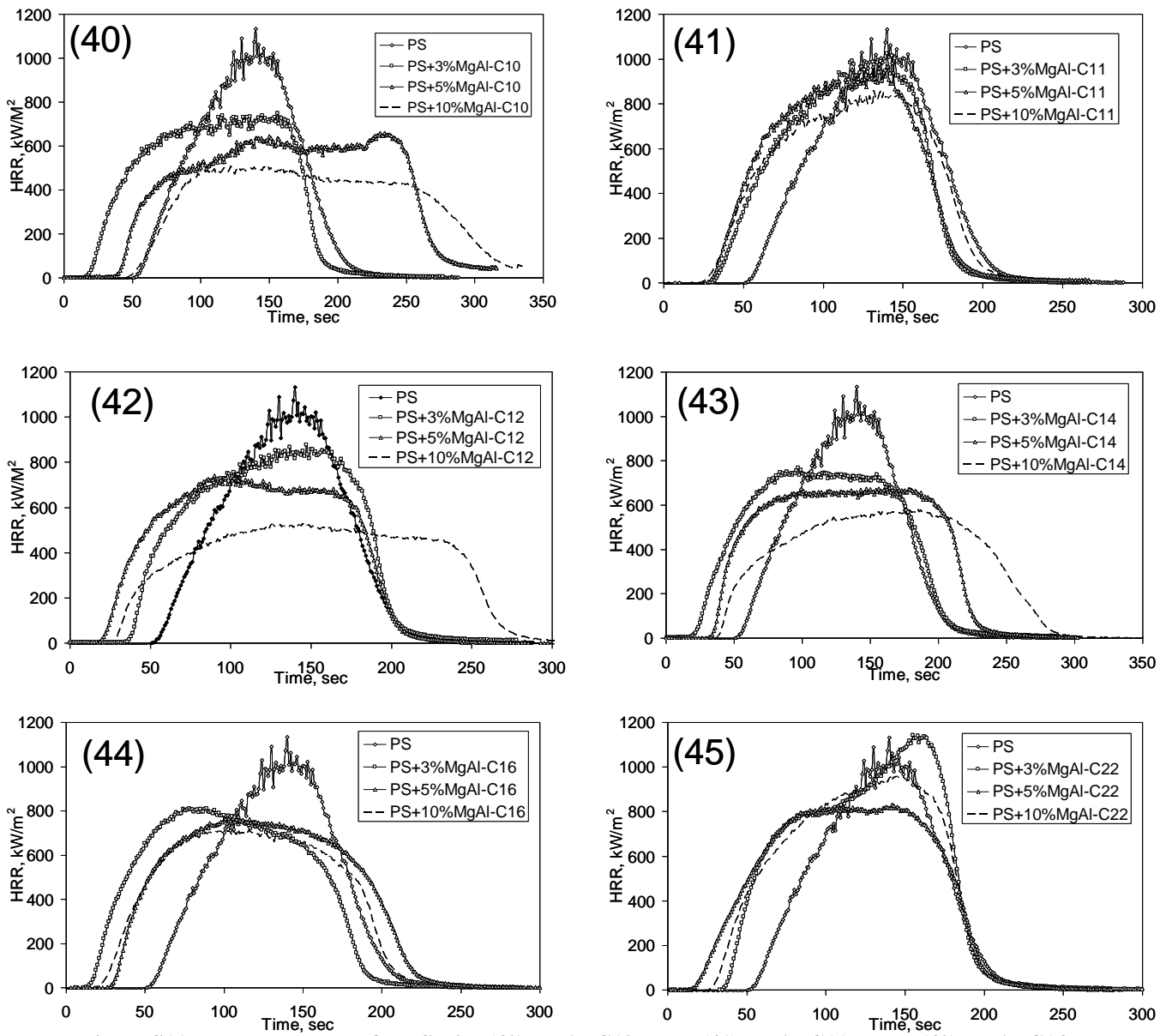


Figure S11 HRR curves for PS with (40) MgAl-C10 LDH, (41) MgAl-C11 LDH, (42) MgAl-C14 LDH, (43) MgAl-C14 LDH, (44) MgAl-C16 LDH and (45) MgAl-C22 LDH at 3, 5 and 10% loadings obtained at 35kW/M²